



Published in final edited form as:

*J Comp Neurol.* 2006 September 20; 498(3): 403–414.

## Dopaminergic Innervation of the Mouse Inner Ear: Evidence for a Separate Cytochemical Group of Cochlear Efferent Fibers

KEITH N. DARROW<sup>1,2</sup>, EMMANUEL J. SIMONS<sup>1,2</sup>, LESLIE DODDS<sup>1</sup>, and M. CHARLES LIBERMAN<sup>1,3,\*</sup>

<sup>1</sup>Eaton-Peabody Laboratory, Massachusetts Eye and Ear Infirmary, Boston, Massachusetts 02114

<sup>2</sup>Program in Speech and Hearing Bioscience and Technology, Division of Health Science and Technology, Harvard and MIT, Cambridge, Massachusetts 02138

<sup>3</sup>Department of Otology and Laryngology, Harvard Medical School, Boston, Massachusetts 02114

### Abstract

Immunostaining mouse cochleas for tyrosine hydroxylase (TH) and dopamine  $\beta$ -hydroxylase suggests that there is a rich adrenergic innervation throughout the auditory nerve trunk and a small dopaminergic innervation of the sensory cell areas. Surgical cuts in the brainstem confirm these dopaminergic fibers as part of the olivocochlear efferent bundle. Within the sensory epithelium, TH-positive terminals are seen only in the inner hair cell area, where they intermingle with other olivocochlear terminals expressing cholinergic markers (vesicular acetylcholine transporter; VAT). Double immunostaining suggests little colocalization of TH and VAT; quantification of terminal volumes suggests that TH-positive fibers constitute only 10–20% of the efferent innervation of the inner hair cell area. Immunostaining of mouse brainstem revealed a small population of TH-positive cells in and around the lateral superior olive. Consistent with cochlear projections, double staining for the cholinergic marker acetylcholinesterase suggested that TH-positive somata are not cholinergic and vice versa. All observations are consistent with the view that a small dopaminergic subgroup of lateral olivocochlear neurons 1) projects to the inner hair cell area, 2) is distinct from the larger cholinergic group projecting there, and 3) may correspond to lateral olivocochlear “shell” neurons described by others (Warr et al. [1997] *Hear. Res* 108:89–111).

### Keywords

tyrosine hydroxylase; colocalization; hearing; feedback control; olivocochlear

---

The lateral olivocochlear (LOC) system forms a neuronal feedback system from the lateral superior olivary complex in the brainstem to the organ of Corti (Guinan et al., 1983). The main peripheral targets of these unmyelinated fibers include the peripheral unmyelinated terminals of auditory nerve afferents in the region under the inner hair cells (IHC; Liberman, 1980); however, a smaller population of synapses on the IHC themselves may also arise from the LOC system (Liberman et al., 1990; Sobkowicz and Slapnick, 1994; Sobkowicz et al., 1997).

The functional role of the LOC system has remained less clear than that of the medial olivocochlear (MOC) system to the outer hair cells (OHC), in large part, because it is only the

---

\*Correspondence to: M. Charles Liberman, PhD, Eaton-Peabody Laboratory, 243 Charles Street, Massachusetts Eye and Ear Infirmary, Boston, MA 02114. E-mail: charles\_liberman@meei.harvard.edu

The first two authors contributed equally to this work.

Grant sponsor: National Institute of Deafness and Other Communication Disorders; Grant number: RO1 DC 00188; Grant number: P30 DC05209.

myelinated axons of the MOC system that are activated when the olivocochlear bundle is electrically stimulated (Gifford and Guinan, 1987), and only the myelinated axons of the MOC system are large enough to record single-fiber responses to sound with glass micropipets (Fex, 1962; Liberman and Brown, 1986). A recent electrophysiological study suggested that the LOC system could be activated indirectly by electrical stimulation of the inferior colliculus (Groff and Liberman, 2003). These authors reported that, depending on electrode placement in the colliculus, the shocks could cause either a slow enhancement or a slow depression of cochlear neural potentials, without changing OHC-based responses such as the cochlear microphonic and distortion product otoacoustic emissions. These slow changes in afferent excitability, with onset time constants greater than 60 seconds, were consistent with expected effects of LOC terminals acting postsynaptically on auditory nerve dendrites. However, the presence of both enhancing and suppressing effects suggested the existence of at least two functional subgroups of LOC fibers.

Such a suggestion for multiple peripheral effects of the LOC system is not unexpected given the apparent plethora of transmitter and neuromodulatory systems it comprises. Over the last 25 years, immunohistochemical evidence has accumulated for the presence of cholinergic,  $\gamma$ -aminobutyric acid (GABA)-ergic, catecholaminergic, and peptidergic transmission in the peripheral terminals of this fiber system (for review, see Eybalin, 1993). Although it is clear that the LOC terminals, as a group, are heterogeneous with respect to their transmitter content, the key question of cytochemical subgroups remains unanswered: are all transmitters colocalized in one class of terminals, or might each transmitter be released by a separate class of fibers? Only a handful of explicit colocalization studies have been performed on the LOC system, and all to date have concluded that all transmitter systems are present in all terminals, i.e., that there is no histological evidence for functional subgroups (Safieddine and Eybalin, 1992; Satake and Liberman, 1996; Maison et al., 2003a), when the transmitters acetylcholine, GABA, and calcitonin gene-related peptide (CGRP) are considered.

The purpose of the present study was to extend the analysis of transmitter colocalization and cytochemical subgroups in the LOC system to include the cochlea's dopaminergic innervation. We use the mouse as an experimental animal in this study, because of an ongoing effort in our laboratory to exploit the availability of mouse lines with targeted deletion of putative LOC-system receptors or neurotransmitters in the inner ear (see, e.g., Maison et al., 2003b) as a useful tool in the analysis of LOC peripheral effects and the functional significance of this neuronal feedback pathway.

## MATERIALS AND METHODS

### Animals, surgery, and histological processing

CBA/CaJ mice between 4 and 9 weeks of age were used in this study. All procedures were approved by the IACUC of the Massachusetts Eye and Ear Infirmary (89-01-006A). For histological processing, animals were anesthetized with ketamine and xylazine, and intravascularly perfused with 4% paraformaldehyde in phosphate-buffered saline (PBS; pH 7.3). In some cases, the fixative also included 0.1% or 0.05% glutaraldehyde. Vascular perfusion was followed by cochlear dissection and perfusion of the cochlear scalae and overnight postfixation in the same fixative. Fixation was followed by decalcification in EDTA. Some ears were then embedded and sectioned, whereas others were dissected and evaluated as whole mounts. For cases to be sectioned, decalcified cochleas were dehydrated in alcohol and embedded in polyester wax, cut at 25  $\mu$ m, and mounted on gel-subbed slides. Prior to staining, the polyester wax sections were treated with HistoClear. Whole-mount ears were carefully dissected into five half-turns with the tectorial membrane and spiral ligament removed prior to immunostaining.

A subset of animals (n = 6) underwent surgery designed to sever the entire olivocochlear bundle (OCB) to one ear. After anesthetization with ketamine and xylazine, a posterior craniotomy was performed and the cerebellum elevated. By using surface landmarks visible on the floor of the fourth ventricle, a microknife was inserted and an incision was made at the sulcus limitans, positioned at the rostrocaudal position of the facial nerve genu and angled in the sagittal plane to sever the OCB to the left ear only; the opposite ear served as control. Animals were allowed to survive for 2 weeks postsurgery (all survived) before brainstems and cochleas were harvested for histological analysis.

A larger subset of animals (n = 17) underwent surgery and a stereotaxic injection of neurotoxin designed to lesion the LOC system unilaterally (Le Prell et al., 2003). After anesthetization with ketamine and xylazine, the mouse was fixed in a Kopf stereotaxic apparatus via snout clamp and ear bars. The skin overlaying the skull was slit and retracted to reveal bregma and lambdoidal sutures. A hole was made over the left lambdoidal suture, and a micropipette filled with a solution of mellitin in saline was inserted into the brainstem by using stereotaxic coordinates derived originally from an atlas of the mouse brain (Franklin and Paxinos, 1997) and modified by trial and error. After the pipette was lowered into the lateral superior olive (LSO) on the right side, an injection of 2  $\mu$ l was made with a 10- $\mu$ l syringe (Hamilton) attached to the micropipette. The opposite ear served as control. Immediately after injection, the scalp was sutured and the animal placed in a padded cage with heat lights for ~1 hour postsurgery. Four weeks later, the brainstem and both cochleas were harvested from each animal.

A final group of (control) animals underwent no surgical procedures before tissue harvest and subsequent immunohistochemistry. Some of these controls (n = 3 animals, 6 olivary complexes) were used to study the brainstem distribution of cholinergic and dopaminergic neurons in the LSO. Others (n = 14 animals, 16 cochleas) were used to study the cochlear distributions. Among the cochleas, nine were doubly immunostained for vesicular acetylcholine transporter (VAT) and tyrosine hydroxylase (TH), and the remaining seven were immunostained for TH only.

For all surgical cases, the brainstems were fixed, sectioned, and stained for acetylcholinesterase (AChE) as described elsewhere (Osen and Roth, 1969). The cochleas were fixed, dissected, and doubly immunostained for VAT and TH (see below). After analysis of the AChE-stained brainstem sections, each surgical case was classified as a hit or a miss: 1/6 OCB sections were successful; however, 10/17 of the LSO lesions were at least partially successful in removing the LOC system unilaterally. All cochleas from both the “hit” and the “miss” cases were analyzed (see below).

## Immunostaining

Primary antibodies were as follows: sheep anti-TH from Calbiochem (La Jolla, CA; 657014, lot No. D19854), rabbit anti-VAT from Sigma (St. Louis, MO; V5387, lot No. 049H4884), and mouse anti-dopamine beta hydroxylase (DBH) from Alpha Diagnostics (DBH11-M, lot No. Xcc0103). The anti-DBH antibody was raised against bovine DBH protein. The anti-TH antibody was raised against native rat pheochromocytoma TH. The specificity of the antibody was assessed by documentation of the locations of immunopositive cells throughout serial sections of the mouse brainstem, compared with that described in the literature and illustrated in an atlas of the mouse brain (Franklin and Paxinos, 1997). The anti-VAT antibody was raised against a synthetic peptide corresponding to the C-terminal of rat VAT (amino acids 512–530). The specificity of the VAT antibody was tested by an adsorption control with a custom peptide from Sigma Genosys, according to the manufacturer's specifications: 1.3 mg peptide was mixed with 1.3 ml water, and 15  $\mu$ l of this solution was added to 500  $\mu$ l of a 1:100 dilution of antibody, vortexed, then put on shaker at room temperature for 4 hours. This preadsorbed solution was diluted (1: 1,000 antibody concentration), and staining of alternate cochlear pieces (with

nonpreadsorbed antibody at the same dilution) was compared: preadsorption eliminated all specific staining.

Cochlear material was immunostained as sections or as dissected whole mounts. Sectioned material (n = 8 cochleas) and some whole mounts (n = 3 cochleas) were singly immunostained for TH (1:1,000) or DBH (1:2,000). After first blocking in 5% normal horse serum (with Triton), sections or whole mounts were incubated in the primary antibody, followed by an appropriate biotinylated secondary antibody (at 1:200). Antibody was visualized in these singly immunostained sections and whole mounts via an ABC kit (Vector Laboratories, Burlingame, CA), followed by chromogen reactions with diaminobenzidine (Adams, 1977). Negative controls were included in each staining run, consisting of sections treated identically except for the lack of the primary antibody incubation.

Double immunostaining for TH and VAT was carried out in cochlear whole mounts only. This approach was applied to nine cochleas from control animals (no surgery) as well as to both cochleas from each of the animals undergoing unilateral OC lesions (see above: n = 23 animals). After the blocking step, cochlear pieces were incubated in the sheep anti-TH (1:500) and the rabbit anti-VAT (1:1,000) overnight, followed by a 1-hour incubation in the VAT secondary (1:400 biotinylated donkey anti-rabbit) and, finally, an overnight incubation in the TH secondary (1:1,000 chicken anti-sheep coupled to AlexaFluor 488) and the VAT tertiary (1:1,000 streptavidin-coupled AlexaFluor 568). Tissue pieces were analyzed and photographed either on a Nikon E-800 microscope equipped with epifluorescence or a Leica confocal microscope.

Immunostaining of brainstem sections for TH was carried out in five cases using the sheep anti-TH (1:500) followed by two AlexaFluor 488-coupled secondary antibodies: chicken anti-goat, followed by goat anti-chicken. For these sections, the immunostaining was followed by histochemical processing for AChE (Osen and Roth, 1969).

### Morphometric analysis

For cochlear whole-mount preparations, cochlear lengths were measured along the pillar heads by computerized planimetry. Cochlear location was converted to frequency according to published maps for mouse (Muller et al., 2005). Cochlear locations in each case corresponding to 10 roughly log-spaced frequency correlates were identified.

Two types of systematic analyses were carried out. In an exhaustive “semiquantitative” analysis, an observer blinded to the surgical histories separately rated the innervation densities for VAT- and TH-positive terminals at each of the 10 points along the cochlear spiral in a set of 36 cochleas, including 10 cochleas ipsilateral to a successful LOC lesion (see above) and 10 opposite-ear controls, seven cochleas ipsilateral to a brainstem injection that missed the LOC and the seven opposite-ear controls, and two cochleas from animals without any brainstem surgery. Separate rating scales were used in IHC and OHC areas. A three-point scale was used for VAT-positive terminals in the OHC area: the observer's task was to estimate the fraction of OHCs with at least one VAT-positive terminal: 3 = 100–66%, 2 = 66–33%, 1 = 33–0%. VAT- and TH-positive terminals in the IHC area were evaluated with a four-point scale: 3 = profuse, 2 = moderate, 1 = sparse, and 0 = none. Each immunostain was separately referenced to its own maximal values; i.e., TH-positive terminals are much rarer than VAT terminals, but maximal density for each would receive a rating “3.”

In a second, more quantitative analysis of four control cochleas (no brainstem surgery), quantification of the relative areas of TH-positive and VAT-positive terminals in the double-immunostained material was carried out by using confocal z-stacks obtained with z-spacing of 0.25  $\mu\text{m}$ . The z-stacks were ported to a 3-D visualization and morphometry software package

(Amira), in which the 3-D volumes of each terminal type were computed: a criterion pixel intensity is selected and the software automatically 1) segments each slice to encircle areas within which the criterion intensity is exceeded, 2) assembles the slices to create 3-D surfaces, and 3) computes the surface area and enclosed volumes. For publication, digital photomicrographs were processed in Photoshop (Adobe Systems): images from the light microscope were processed with gamma correction and unsharp mask; images from the confocal were processed with a gamma correction only.

## RESULTS

### Analysis of cochlear projections

**Single-staining results**—To differentiate adrenergic from dopaminergic innervation, cochleas were immunostained with either TH or DBH. Because TH catalyzes the first step in the biosynthetic pathway common to dopamine and norepinephrine, whereas DBH catalyzes the conversion of dopamine to norepinephrine, adrenergic fibers are immunopositive for both TH and DBH, whereas dopaminergic fibers should be TH positive and DBH negative.

TH immunoreactivity was seen in all cochleas examined as sectioned material ( $n = 8$ ). Analysis of 70 immunostained sections revealed beaded TH-positive fibers throughout the modiolus and osseous spiral lamina (e.g., Fig. 1A). A few of the TH-positive fibers were clearly associated with blood vessels, spiraling around their circumference; however the majority were not, taking an uncoiled trajectory through the neuropil of the modiolar region (e.g., solid arrow in Fig. 1A). In many sections (59/70), immunopositive puncta were also clearly seen in the inner spiral bundle (ISB), in the region under the IHC (e.g., within the dashed circle in Fig. 1B). Labeled swellings were never seen in the OHC area.

Sections stained with anti-DBH also showed immunopositive beaded fibers in the modiolus and osseous spiral lamina (OSL); however, immunopositive puncta were never seen in the ISB (50 immunostained sections were analyzed, with multiple views of the organ of Corti in each section). Together, these observations suggest there is a rich adrenergic innervation of the modiolus, as previously reported (see, e.g., Spoenclin and Lichtensteiger, 1966; Terayama et al., 1966; Hozawa et al., 1989), and a sparse dopaminergic innervation of the cochlear epithelium.

To assess better the morphology of TH-positive fibers in the organ of Corti, several cochleas were dissected and immunoreacted as whole mounts. In this whole-mount material, immunopositive swellings were clearly visible within the ISB beneath the IHC (e.g., open arrows in Fig. 1C). In some material, the thin axonal processes connecting the en passant swellings were also immunostained. In all cases, the total volume of TH-positive puncta in the ISB was significantly less than that seen when similar material is immunostained for SNAP25, synaptophysin, or other markers for all olivocochlear efferent terminals (Maison et al., 2003a; and see below). However, individual TH-positive swellings were darkly labeled, suggesting that incomplete labeling was not the cause of the small numbers of immunopositive terminals.

**Double-staining results**—Previous immunohisto-chemical analysis of the olivocochlear innervation of the mouse cochlea suggested that the vast majority of olivocochlear terminals in the ISB express the cholinergic marker VAT and also colocalize a GABAergic marker as well as the neuropeptide CGRP (Maison et al., 2003a). To address whether TH-positive fibers in the organ of Corti represent a distinct fiber group or a subset of the cholinergic/GABAergic/CGRPergic population, we double-stained a number of cochlear whole-mount preparations for TH and VAT.

The analysis of these double-stained cochleas suggests that TH-positive fibers in the organ of Corti represent a small, separate population; i.e., the small numbers of TH-positive fibers in the ISB do not generally express VAT, and the large numbers of VAT-positive fibers in the ISB do not generally express TH. The merged confocal image in Figure 2A illustrates the point: in the ISB, VAT-positive (red) terminals greatly outnumber the TH-positive (green) terminals, and the OHC area shows a robust VAT-positive innervation, whereas no TH immunostaining is visible.

Most of the TH staining in the ISB area appears to be complementary to the VAT staining (e.g., arrow), but the occasional yellow profile suggests some colocalization. However, much of this apparent colocalization in the merged projections arises from superposition of TH and VAT immunoreactivity from different z planes. This superposition is illustrated in Figure 3: for the two yellow terminals in the projection view (Fig. 3A), examination of the single z plane from which the TH signal arises (Fig. 3B) shows no colocalization in either terminal. The signal in the VAT channel was from other terminals at a different focal level (not shown).

To assess whether there is any spatial segregation of TH-positive and VAT-positive terminals in the IHC area, we obtained confocal z-stacks and viewed the projections in all three orthogonal planes. As illustrated by the xy, xz, and yz projections of one such stack (Fig. 2A-C, respectively), there is no clear evidence of any spatial segregation. Note that comparison of all three projections reveals that the cluster of apparent colocalization in the yz projection (Fig. 2C) arises largely because of the superposition of green and red pixels from different z-levels. Similar stacks were obtained and examined from all regions along the cochlear spiral in numerous cases: no clearcut evidence for spatial segregation was seen.

To quantify the ratio of TH-positive to VAT-positive profiles in the IHC area, as well as the fraction of terminals expressing both markers, we performed 3-D morphometry on these confocal z-stacks with a software package (Amira) that allows rapid derivation and measurement of 3-D isosurfaces enclosing all voxels exceeding user-specified intensities (e.g., Fig. 2D-F). Based on a sample of three cochlear regions in one representative ear (at positions about 25%, 50%, and 75% from the base), the volume fraction of all labeled terminals in the ISB that were TH-positive was 23.4%, 9.1%, and 14.2%, respectively. More than half of these TH-positive terminals did not colocalize VAT: the volume fraction of those TH-positive terminals that were not also VAT positive was 77%, 94%, and 58%, respectively. Qualitative evaluation of dozens of other well-stained cochleas suggests that these values are representative.

Semiquantitative evaluation of all cochlear regions of all double-stained cochleas suggested that there is no apical-basal gradient of TH immunoreactivity along the cochlear spiral (Fig. 4B); the slight gradient for VAT staining (Fig 4A; broad midcochlear peak with slight dropoff toward the base and apex) is consistent with a prior quantitative analysis of LOC innervation density in mouse (Maison et al., 2003a). Note that the rating scale for each immunostain was normalized to its own maximal density, so differences in absolute terminal densities between VAT and TH immunostains are not captured by this analysis.

An additional feature of the difference between the distributions of VAT- and TH-positive terminals is captured by the error bars in Figure 4. Whereas the distribution of VAT-immunoreactive terminals appears continuous, and the density of VAT-positive terminals in one cochlea changes slowly with cochlear position; the TH innervation is discontinuous, such that a localized region of high terminal density can be flanked by regions with no immunoreactivity (Fig. 5). It is possible that each “hot spot” of TH innervation corresponds to the terminal arbor of a single parent fiber.

## Analysis of brainstem origins

**Brainstem lesions**—To investigate the brainstem origins of the TH-positive fibers in the modiolus and the organ of Corti, we lesioned the olivocochlear system in two different ways. In one set of experiments, we cut the OCB at the floor of the fourth ventricle near the sulcus limitans. At this lateral position, the cuts can interrupt all fibers of the LOC and MOC systems (Lieberman and Gao, 1995). In a second, larger set of experiments, we selectively lesioned the LOC system unilaterally, by stereotaxic injection of a neurotoxin (Le Prell et al., 2003). Because the projections of the LOC are almost entirely ipsilateral, this lesion should selectively disrupt the LOC innervation to only one cochlea, leaving the other ear as a control. The success of the lesions was evaluated by examination of brainstem sections stained for AChE, which reveals the olivocochlear bundle as well as the cholinergic cells of the MOC and LOC systems in the superior olivary complex (SOC).

The most successful OC bundle cut is shown in Figure 6B: the VAT staining shows the marked reduction in efferent innervation of OHC and the IHC area; the green channel shows a complete loss of TH-positive terminals in the ISB area, without obvious diminution of the profuse TH-positive innervation of the osseous spiral lamina by beaded fibers. These observations are consistent with the view that the TH-positive innervation of the organ of Corti arises from the olivocochlear system, whereas the beaded fibers in the lamina are part of the adrenergic innervation arising from the superior cervical ganglion (Spoendlin and Lichtensteiger, 1966; Terayama et al., 1966; Hozawa et al., 1989).

Unilateral LOC lesions also caused loss of both VAT and TH immunoreactivity in the ipsilateral IHC area, but without affecting the VAT-positive terminals on OHC (or the TH-positive beaded fibers in the osseous spiral lamina) in either ear, which is consistent with the view that the OHC innervation arises exclusively from the MOC system. Confocal projections of efferent terminals in the organ of Corti from a representative “LOC hit” case (Fig. 6D) can be compared with the place-matched cochlear region from the ear opposite the lesion (Fig. 6C). Results of the semiquantitative analysis of all cochleas from the LOC lesion study, by an observer blind to the surgical history of each case, further confirm the view that both the VAT- and the TH-positive terminals in the IHC area originate from the LOC cells located in the ipsilateral LSO, whereas the VAT-positive terminals in the OHC area arise from MOC cells located more medially in the brainstem. For both stains, the differences in density ratings in the IHC area for the lesioned vs. control (opposite) ears was statistically significant by two-way ANOVA (TH:  $P = 0.001$ ,  $F = 12.755$ ; VAT:  $P < 0.000$ ,  $F = 18.733$ ), whereas there was no change in VAT-positive terminals in the OHC area ( $P = 0.595$ ,  $F = 0.288$ ; data not shown). For those cases in which the neurotoxin injection missed the LOC, differences in TH and VAT terminal densities between the injected and control sides were not significant by two-way ANOVA (TH:  $P = 0.206$ ,  $F = 1.683$ ; VAT:  $P = 0.245$ ,  $F = 1.398$ ; data not shown).

**Brainstem immunostaining**—To confirm and clarify the origins of this putative dopaminergic innervation of the mouse cochlea, we examined immunostained sections of the olivary complex for the presence or absence of TH immunoreactivity. As illustrated by the micro-graphs in Figure 7, there were small numbers of immunoreactive cell bodies located within or immediately around the LSO. In two cases, we evaluated serial sections through the LSO and counted the total number of TH-positive cell bodies on both sides: we found a total of only 62 TH-positive cells in the four LSOs combined. Among these, 47 were in the “shell” region on the outer perimeter of the LSO (Warr et al., 1997) and only 15 were within the LSO itself. In one case, among the seven “intrinsic” neurons found, six of seven were in the (high-frequency) medial limb and only one was in the (low-frequency) lateral limb. In the other case, they were more evenly distributed. As shown in Figures 7 and 8, TH-positive shell neurons tended to be found lateral to the LSO.

To confirm further the general lack of colocalization of cholinergic and dopaminergic markers seen in the cochlea, we doubly stained brainstem sections for AChE (histo-chemically) and TH (immunohistochemically). As shown in Figure 8, there appeared to be little overlap: cell bodies and axons that were TH positive were not strongly positive for the cholinergic marker and vice versa.

## DISCUSSION

### Cochlear terminations of dopaminergic neurons

The two major catecholamine neurotransmitters, dopamine and noradrenaline, are both present in fiber systems projecting to the inner ear. As will be described below, evidence suggests that the former is present in fibers originating in the SOC and comprising part of the olivocochlear bundle, whereas the latter is found in fibers originating in the superior cervical ganglion and making up the sympathetic innervation of the inner ear.

Since the 1960s, histochemical techniques at both light and electron microscopic levels have been used to identify an adrenergic innervation of the inner ear in cat, guinea pig, rabbit, and squirrel monkey; this sympathetic innervation originates in the superior cervical ganglion projects exclusively to the ipsilateral ear and terminates in a plexus of vessel-associated and vessel-independent fibers in both the modiolus and the osseous spiral lamina (Terayama et al., 1966; Spoendlin and Lichtensteiger, 1967; Hozawa et al., 1989). There is widespread agreement among neuroanatomical studies that these adrenergic fibers do not enter the organ of Corti; rather, they appear to make synaptic contact with the fibers of the auditory nerve in the region near the habenula perforata (Densert and Flock, 1974), in all mammals, as well as within the spiral ganglion in monkey (Hozawa and Kimura, 1990). The adrenergic fibers presumably correspond in the present study to the rich innervation of the osseous spiral lamina and modiolus by beaded TH-positive fibers.

Since the 1980s, immunohistochemical evidence has accumulated for a population of dopaminergic neurons that originates in the SOC and, as part of the olivocochlear bundle, projects to the ISB, where the fibers send branches or en passant swellings to contact unmyelinated dendrites of the auditory nerve (d'Aldin et al., 1995). Dopamine is a precursor of noradrenaline, so both fiber types are immunopositive for tyrosine hydroxylase (TH), whereas only adrenergic fibers are immunopositive for DBH. Thus, the presence of TH-positive, DBH-negative fibers in the organ of Corti has provided anatomical evidence for a dopaminergic innervation in the guinea pig (see, e.g., Jones et al., 1987; Niu and Canlon, 2002; Mulders and Robertson, 2004) and now in the mouse (present study).

In the present study, we showed that surgical interruption of the olivocochlear bundle at the floor of the fourth ventricle, or stereotaxic destruction of the LSO complex, resulted in loss of TH immunolabeling in the organ of Corti, without reducing the rich plexus of TH-positive fibers in the osseous spiral lamina (Figs. 4, 6). These observations are consistent with the idea that the adrenergic innervation of the modiolus does not extend into the organ of Corti and that the TH-positive fibers in the organ of Corti are part of the olivocochlear efferent system, in particular part of the LOC system.

All studies of TH-positive fibers in the organ of Corti agree that such fibers are restricted to the ISB and tunnel spiral bundle; i.e., they do not appear to project to the OHC region. Two previous studies in the guinea pig address the question of an apex-to-base gradient in the density of the TH-positive innervation (Niu and Canlon, 2002; Mulders and Robertson, 2004). Although neither previous study quantified the gradient, both suggest that TH-positive terminals are more numerous in the basal turn and sparse in the apical turn. These results in guinea pig are nominally in contrast to those from the mouse, in which the distribution of TH-



positive terminals was quite uniform from base to apex (Fig. 4). However, the fact that the mouse is a high-frequency mammal and that the apicalmost point on its cochlear spiral is tuned to ~4.0 kHz (Muller et al., 2005), which in the guinea pig corresponds to the upper basal turn (Tsuji and Liberman, 1997), suggests the hypothesis that a dopaminergic innervation is important for high-frequency regions of the mammalian cochlea in an absolute (>3 kHz), rather than a relative (apex vs. base) sense.

No previous study of the dopaminergic innervation of the organ of Corti has addressed the important issues of 1) colocalization of TH with other efferent-terminal markers or 2) the relative numbers of TH-positive terminals compared with the total numbers of olivocochlear terminals in the IHC area. In the present study, we found the volume of TH-positive terminals to be only 10–25% of the volume of VAT-positive terminals. We used VAT, a cholinergic marker, because a previous study in mouse (Maison et al., 2003a) found 1) that cholinergic, GABAergic and peptidergic markers were all colocalized in terminals of the ISB and 2) that VAT-positive terminal areas were similar to terminal areas immunostained by SNAP25, a marker of synaptic vesicles expected to label all efferent terminals. However, no double-staining studies were performed to determine whether a small VAT-negative/SNAP25-positive subset existed.

Combining the results of the present study with those of the previous colocalization study in mouse suggests that there may be two cytochemical subgroups within the LOC system, one large group of fibers that colocalizes ACh, GABA, and CGRP and a smaller group of fibers that may be solely or largely dopaminergic and that projects mainly to the IHC area throughout the cochlear spiral. Such a view is not inconsistent with a previous colocalization study in guinea pig and rat, which also concluded that, in the cochlear terminals of OC fibers, ACh, CGRP, and opioid peptides were also extensively colocalized (Safieddine and Eybalin, 1992).

The present study showed that a small fraction of TH-positive terminals also showed some VAT immunoreactivity, suggesting that there is not an absolute distinction between dopaminergic and cholinergic neurons; rather, there might be a continuum of expression levels. Nevertheless, the degree of separation between the dopaminergic innervation and the cholinergic innervation is much more robust than that between the cholinergic and GABAergic, for example, for which the expression patterns in cochlear terminals overlapped completely (Maison et al., 2003b).

### Central origins of dopaminergic neurons

The data on TH immunoreactivity in the LSO are largely consistent with the view afforded by evaluation of the immunostained cochlea in both mouse (present study) and guinea pig (Mulders and Robertson, 2004). For the mouse, we found a small number of TH-positive neurons in and around the LSO: an average of only 16 per side. The estimated total number of LOC cells in mouse ( $n = 310$ ), derived from a study of retrograde cochlear transport of horseradish peroxidase (HRP; Campbell and Henson, 1988), suggests that the TH-positive cell bodies make up ~5% of the LOC system. Such an estimate is not inconsistent with the estimates derived from comparison of the cochlear innervation densities, although they suggest that the TH-positive cells might tend to be more highly branched than the cholinergic neurons (an inference that is also consistent with other lines of argument presented below).

In the guinea pig, the numbers of TH-positive LSO cells are greater, in both absolute and relative terms; however, the idea that they constitute a small fraction of the total LOC system is supported by two studies. One group (Mulders and Robertson, 2004) counted TH-positive cells in alternate sections of two LSO from guinea pig after labeling LOC neurons with a retrograde tracer injected into the cochlea. They report that only a “small number” of LOC

cells (i.e., tracer-positive cells in the LSO region) was TH positive but that almost all of the TH-positive cells were also tracer positive (i.e., part of the olivocochlear system) and that they tended to be found “at the edge of the LSO.” Overall, 92 TH-positive cells were counted in one animal, and 111 in another, in every second section. If we multiply by 2 (ignoring the double-count correction, which must be significant here), we get at most ~200 TH-positive neurons. According to another retrograde label study, the total LOC population in one guinea pig LSO is ~1,300 (Aschoff and Ostwald, 1987); thus, the TH-positive subset constitutes just over 15%. In another study of LOC cells identified by retrograde transport from the cochlea, the total number of TH-positive LOC cells was found to be ~155 per side, and the fraction of total LOC neurons that this number represented was estimated at 35% (Niu et al., 2004).

These observations from single-antigen immunolabeling coupled with retrograde transport to identify LOC neurons are hard to square with data from triple immunostaining of LSO neurons for cholinergic (anti-ChAT), GABAergic (anti-GAD), and catecholaminergic (anti-TH) markers by Safeiddine and colleagues (1997), who studied rats and guinea pigs. These authors, who did not use retrograde tracing techniques to identify OC neurons directly, concluded that 94% of neurons in the LSO regions that were immunopositive for ChAT were also immunopositive for GAD and TH. One way to resolve the two sets of studies is to hypothesize that large numbers of cholinergic LSO cells are not part of the OC system. However, that hypothesis is not consistent with reports of Vetter and colleagues (1991) for the rat.

The majority of TH-positive neurons in the present study were located near the edges, or just outside the LSO borders, and thus may correspond to LOC “shell” neurons. As extensively studied by Warr and colleagues (Warr et al., 1997; Sanchez-Gonzalez et al., 2003; Warr and Boche, 2003), LOC cochlear projections appear to be of two major subtypes: 1) a large population of small intrinsic neurons, located within the LSO proper, and 2) a smaller population of shell neurons, located around the LSO border, which tend to be larger. In the rat, shell neurons are outnumbered by intrinsic neurons by ~10:1; data are not available for mouse (Sanchez-Gonzalez et al., 2003). Anterograde tracer studies further suggest that shell neurons give rise to highly branched peripheral projections, which may spiral to innervate more than half of the cochlea's length, in contrast to intrinsic LOC neurons, which give rise to projections with more restricted trajectories within the ISB (Brown, 1987).

Thus, both by cell location and by cell proportions, the present data are consistent with the idea that dopaminergic cochlear innervation arises largely from LOC shell neurons. However, it does not appear likely that all shell neurons are dopaminergic. Vetter and colleagues (1991) report that about half of the shell LOC neurons, identified by retrograde HRP transport from the cochlea, immuno-stain for cholinergic or GABAergic markers; whereas about half stain for neither. If half of the shell neurons in rat are dopaminergic, and if shell neurons make up about 10% of the total number of LOC cells in rat (Sanchez-Gonzalez et al., 2003), then dopaminergic LOC cells would constitute about 5% of the total LOC somata, closely corresponding to the estimates derived above for mouse. If, furthermore, these relatively rare dopaminergic shell neurons are particularly highly branched relative to the more common intrinsic (cholinergic) neurons, the observed ratios of immunolabeled dopaminergic to cholinergic terminals in the ISB should be significantly amplified, as indeed they were (to values of 9–24%).

### **Functional significance of a cochlear dopaminergic innervation**

The evidence that the LOC efferent system contains a functional dopaminergic innervation now derives from many sources. Beyond the histochemical and immunohistochemical evidence described in the previous section, there is biochemical evidence showing electrically evoked release of dopamine from the cochlea, which can be blocked by tetrodotoxin (Gaborjan et al., 1999); there is pharmacological evidence showing that cochlear dopamine perfusion

decreases spontaneous and sound-evoked activity in the auditory nerve (Ruel et al., 2001); and there are RT-PCR data showing cochlear expression of several dopamine receptors in the cochlea (Karadaghy et al., 1997), although there are currently no data on the tissue localization of such receptors.

A recent electrophysiological study suggested that electrical activation of the LOC system by shocking the inferior colliculus can either decrease or increase the amplitude of the cochlear neural potentials, depending on where the stimulus was applied within the colliculus (Groff and Liberman, 2003). Because these neural effects were seen without changes in OHC function (i.e., DPOAE magnitude), it was suggested that they arise from interactions between the LOC terminals and their peripheral targets the auditory nerve fibers and/or IHC. It was further suggested that there might be two functional subgroups of neurons within the LOC. Data from the present study suggest the obvious possibility that the suppressive effects arise by selective activation of the dopaminergic system, whereas the excitatory effects arise by activation of the system that colocalizes ACh, GABA, and CGRP.

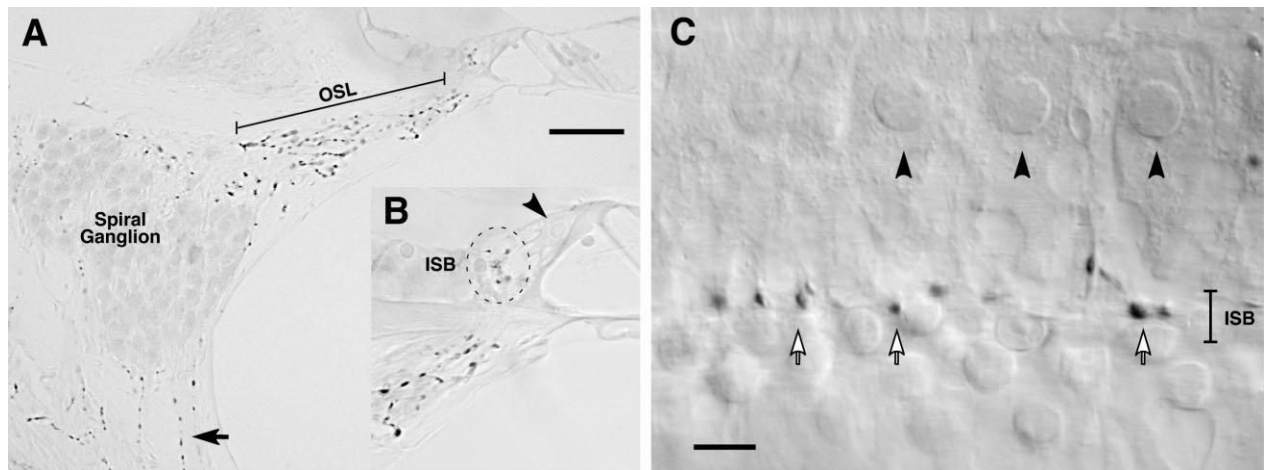
One interesting hypotheses concerning the functional significance of this dopaminergic innervation is that it acts to minimize glutamate-like excitotoxicity at the IHC/afferent synapse after acoustic overexposure (Pujol and Puel, 1999). This excitotoxic effect of acoustic overstimulation is seen as a marked swelling of afferent dendrites during the acute phase of the response to the insult (Liberman and Mulroy, 1982; Robertson, 1983). It has been shown that cochlear perfusion of the dopamine-receptor blocker eticlopride can result in a similar type of dendritic vacuolization under the IHC (Ruel et al., 2001) and that acoustic overstimulation can lead to depletion of TH immunoreactivity in the cochlea (Niu and Canlon, 2002). It has further been shown that selective destruction of the LOC system in mouse by the same types of stereotaxic injections used in the present study leads to an enhanced vulnerability to the acute effects of acoustic overexposure (Darrow et al., 2006); incorporating results from the present study would suggest that this protective effect of the LOC system arises from the small, cytochemically distinct population of dopaminergic fibers.

## LITERATURE CITED

- Adams JC. Technical considerations on the use of horseradish peroxidase as a neuronal marker. *Neuroscience* 1977;2:141–145. [PubMed: 917271]
- Aschoff A, Ostwald J. Different origins of cochlear efferents in some bat species, rats, and guinea pigs. *J Comp Neurol* 1987;264:56–72. [PubMed: 3680624]
- Brown MC. Morphology of labeled efferent fibers in the guinea pig cochlea. *J Comp Neurol* 1987;260:605–618. [PubMed: 3611413]
- Campbell JP, Henson MM. Olivocochlear neurons in the brainstem of the mouse. *Hear Res* 1988;35:271–274. [PubMed: 3198515]
- d'Aldin CE, Jahn AF, Puel JL, Charachon G, Ladrech S, Renard N, Pujol R. Synaptic connections and putative functions of the dopaminergic innervation of the guinea pig cochlea. *Eur Arch Otorhinolaryngol* 1995;252:270–274. [PubMed: 7576583]
- Darrow KN, Maison SF, Liberman MC. Selective removal of lateral olivocochlear efferents causes increased vulnerability to acute acoustic injury. Abstracts of the XXIXth ARO Midwinter Meeting 2006;29:297.
- Densert O, Flock A. An electron-microscopic study of adrenergic innervation in the cochlea. *Acta Otolaryngol* 1974;77:185–197. [PubMed: 4819031]
- Eybalin M. Neurotransmitters and neuromodulators of the mammalian cochlea. *Physiol Rev* 1993;73:309–373. [PubMed: 8097330]
- Fex J. Auditory activity in centrifugal and centripetal cochlear fibers in cat. *Acta Physiol Scand* 1962;55:2–68. [PubMed: 14480277]

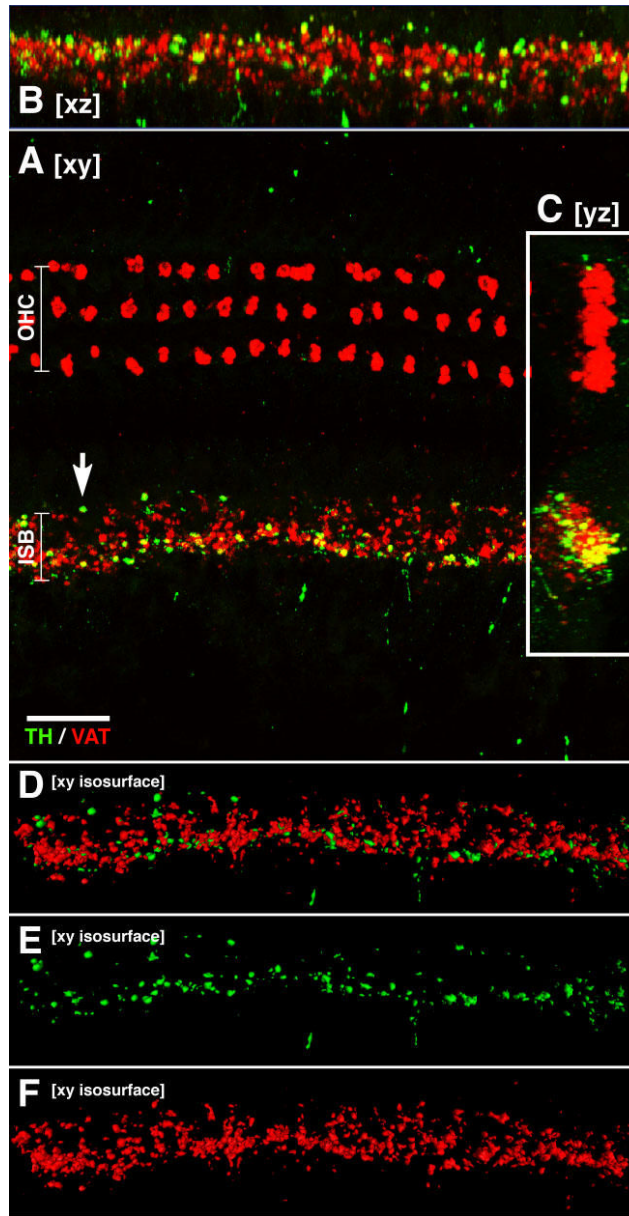
- Franklin, KBJ.; Paxinos, G. The mouse brain in stereotaxic coordinates. Academic Press; New York: 1997.
- Gaborjan A, Lendvai B, Vizi ES. Neurochemical evidence of dopa-mine release by lateral olivocochlear efferents and its presynaptic modulation in guinea-pig cochlea. *Neuroscience* 1999;90:131–138. [PubMed: 10188940]
- Gifford ML, Guinan JJ Jr. Effects of electrical stimulation of medial olivocochlear neurons on ipsilateral and contralateral cochlear responses. *Hear Res* 1987;29:179–194. [PubMed: 3624082]
- Groff JA, Liberman MC. Modulation of cochlear afferent response by the lateral olivocochlear system: activation via electrical stimulation of the inferior colliculus. *J Neurophysiol* 2003;90:3178–3200. [PubMed: 14615429]
- Guinan JJ Jr, Warr WB, Norris BE. Differential olivocochlear projections from lateral vs. medial zones of the superior olivary complex. *J Comp Neurol* 1983;221:358–370. [PubMed: 6655089]
- Hozawa J, Kimura RS, Takahashi S. Sympathetic nervous system in the guinea pig cochlea. *Ear Res Jpn* 1989;20:111–112.
- Hozawa K, Kimura RS. Cholinergic and noradrenergic nervous systems in the cynomolgus monkey cochlea. *Acta Otolaryngol* 1990;110:46–55. [PubMed: 1974732]
- Jones N, Fex J, Altschuler RA. Tyrosine hydroxylase immunoreactivity identifies possible catecholaminergic fibers in the organ of corti. *Hear Res* 1987;30:33–38. [PubMed: 2890616]
- Karadaghy AA, Lasak JM, Chomchai JS, Khan KM, Drescher MJ, Drescher DG. Quantitative analysis of dopamine receptor messages in the mouse cochlea. *Brain Res Mol Brain Res* 1997;44:151–156. [PubMed: 9030711]
- Le Prell CG, Shore SE, Hughes LF, Bledsoe SC Jr. Disruption of lateral efferent pathways: functional changes in auditory evoked responses. *J Assoc Res Otolaryngol* 2003;4:276–290. [PubMed: 12943378]
- Liberman MC. Efferent synapses in the inner hair cell area of the cat cochlea: An electron microscopic study of serial sections. *Hear Res* 1980;3:189–204. [PubMed: 7440423]
- Liberman MC, Brown MC. Physiology and anatomy of single olivocochlear neurons in the cat. *Hear Res* 1986;24:17–36. [PubMed: 3759672]
- Liberman MC, Gao WY. Chronic cochlear de-efferentation and susceptibility to permanent acoustic injury. *Hear Res* 1995;90:158–168. [PubMed: 8974993]
- Liberman, MC.; Mulroy, MJ. Acute and chronic effects of acoustic trauma: Cochlear pathology and auditory nerve pathophysiology. In: Hamernik, RP.; Henderson, D.; Salvi, R., editors. *New perspectives on noise-induced hearing loss*. Raven Press; New York: 1982. p. 105-136.
- Liberman MC, Dodds LW, Pierce S. Afferent and efferent innervation of the cat cochlea: quantitative analysis with light and electron microscopy. *J Comp Neurol* 1990;301:443–460. [PubMed: 2262601]
- Maison SF, Adams JC, Liberman MC. Olivocochlear innervation in mouse: immunocytochemical maps, crossed vs. uncrossed contributions and colocalization of ACh, GABA, and CGRP. *J Comp Neurol* 2003a;455:406–416. [PubMed: 12483691]
- Maison SF, Emeson RB, Adams JC, Luebke AE, Liberman MC. Loss of alpha CGRP reduces sound-evoked activity in the cochlear nerve. *J Neurophysiol* 2003b;90:2941–2949. [PubMed: 12904337]
- Mulders WH, Robertson D. Dopaminergic olivocochlear neurons originate in the high frequency region of the lateral superior olive of guinea pigs. *Hear Res* 2004;187:122–130. [PubMed: 14698093]
- Muller M, von Hunerbein K, Hoidis S, Smolders JW. A physiological place-frequency map of the cochlea in the CBA/J mouse. *Hear Res* 2005;202:63–73. [PubMed: 15811700]
- Niu X, Canlon B. Activation of tyrosine hydroxylase in the lateral efferent terminals by sound conditioning. *Hear Res* 2002;174:124–132. [PubMed: 12433403]
- Niu X, Bogdanovic N, Canlon B. The distribution and the modulation of tyrosine hydroxylase immunoreactivity in the lateral olivocochlear system of the guinea-pig. *Neuroscience* 2004;125:725–733. [PubMed: 15099686]
- Osen KK, Roth K. Histochemical localization of cholinesterases in the cochlear nuclei of the cat with notes on the origin of acetylcholinesterase-positive afferents and the superior olive. *Brain Res* 1969;16:165–185. [PubMed: 5348847]

- Pujol R, Puel JL. Excitotoxicity, synaptic repair and functional recovery in the mammalian cochlea: a review of recent findings. *Ann N Y Acad Sci* 1999;884:249–254. [PubMed: 10842598]
- Robertson D. Functional significance of dendritic swelling after loud sounds in the guinea pig cochlea. *Hear Res* 1983;9:263–278. [PubMed: 6841283]
- Ruel J, Nouvian R, Gervais d'Aldin C, Pujol R, Eybalin M, Puel JL. Dopamine inhibition of auditory nerve activity in the adult mammalian cochlea. *Eur J Neurosci* 2001;14:977–986. [PubMed: 11595036]
- Safieddine S, Eybalin M. Triple immunofluorescence evidence for a coexistence of acetylcholine, enkephalins and calcitonin gene-related peptide within efferent (olivocochlear) neurons of rats and guinea pigs. *Eur J Neurosci* 1992;4:921–992.
- Safieddine S, Prior AM, Eybalin M. Choline acetyltransferase, glutamate decarboxylase, tyrosine hydroxylase, calcitonin gene-related peptide and opioid peptides coexist in lateral efferent neurons of rat and guinea-pig. *Eur J Neurosci* 1997;9:356–367. [PubMed: 9058055]
- Sanchez-Gonzalez MA, Warr WB, Lopez DE. Anatomy of olivocochlear neurons in the hamster studied with FluoroGold. *Hear Res* 2003;185:65–76. [PubMed: 14599694]
- Satake M, Liberman MC. Morphological subclasses of lateral olivocochlear terminals? Ultrastructural analysis of inner spiral bundle in cat and guinea pig. *J Comp Neurol* 1996;371:621–632. [PubMed: 8841914]
- Sobkowicz HM, Slapnick SM. The efferents interconnecting auditory inner hair cells. *Hear Res* 1994;75:81–92. [PubMed: 8071157]
- Sobkowicz HM, Slapnick SM, Nitecka LM, August BK. Compound synapses within the GABAergic innervation of the auditory inner hair cells in the adolescent mouse. *J Comp Neurol* 1997;377:423–442. [PubMed: 8989656]
- Spoendlin H, Lichtensteiger W. The adrenergic innervation of the labyrinth. *Acta Otolaryngol* 1966;61:423–434. [PubMed: 5915897]
- Spoendlin H, Lichtensteiger W. The sympathetic nerve supply to the inner ear. *Arch Klin Exp Ohren-Nasen- Kehlkopfheilk* 1967;189:346–359.
- Terayama Y, Holz E, Beck C. Adrenergic innervation of the cochlea. *Ann Otol Rhinol Laryngol* 1966;75:69–86. [PubMed: 4160202]
- Tsuji J, Liberman MC. Intracellular labeling of auditory nerve fibers in guinea pig: central and peripheral projections. *J Comp Neurol* 1997;381:188–202. [PubMed: 9130668]
- Vetter DE, Adams JC, Mugnaini E. Chemically distinct rat olivocochlear neurons. *Synapse* 1991;7:21–43. [PubMed: 1706537]
- Warr WB, Boche JE. Diversity of axonal ramifications belonging to single lateral and medial olivocochlear neurons. *Exp Brain Res* 2003;153:499–513. [PubMed: 14557913]
- Warr WB, Boche JB, Neely ST. Efferent innervation of the inner hair cell region: origins and terminations of two lateral olivocochlear systems. *Hear Res* 1997;108:89–111. [PubMed: 9213126]

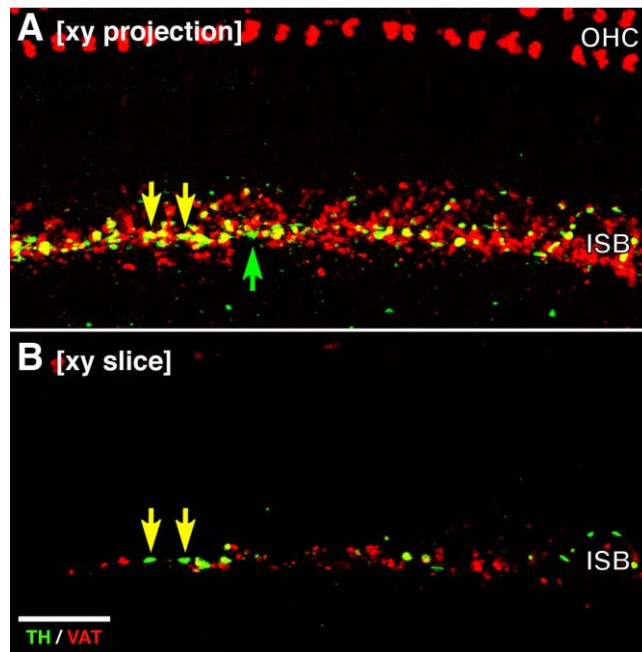


**Fig. 1.**

TH immunostaining of cochlear sections (A) and whole mounts (B) reveals a TH-positive innervation of the modiolus, osseous spiral lamina, and organ of Corti. **A:** Immunostained cochlear section from the upper basal turn shows TH-positive beaded fibers in the osseous spiral lamina (OSL) and modiolus (e.g., solid arrow). **B** shows a higher magnification view of the immunostained puncta in the inner spiral bundle (ISB). The position of the inner hair cell nucleus is indicated by the arrowhead. This image is from the upper basal turn. **C:** Immunostained cochlear whole mount shows strings of TH-positive en passant swellings (three are indicated by open arrows) in the ISB beneath the inner hair cells. Nuclei of three adjacent inner hair cells are indicated by the arrowheads. Scale bars = 50  $\mu\text{m}$  in A; 5  $\mu\text{m}$  in C.

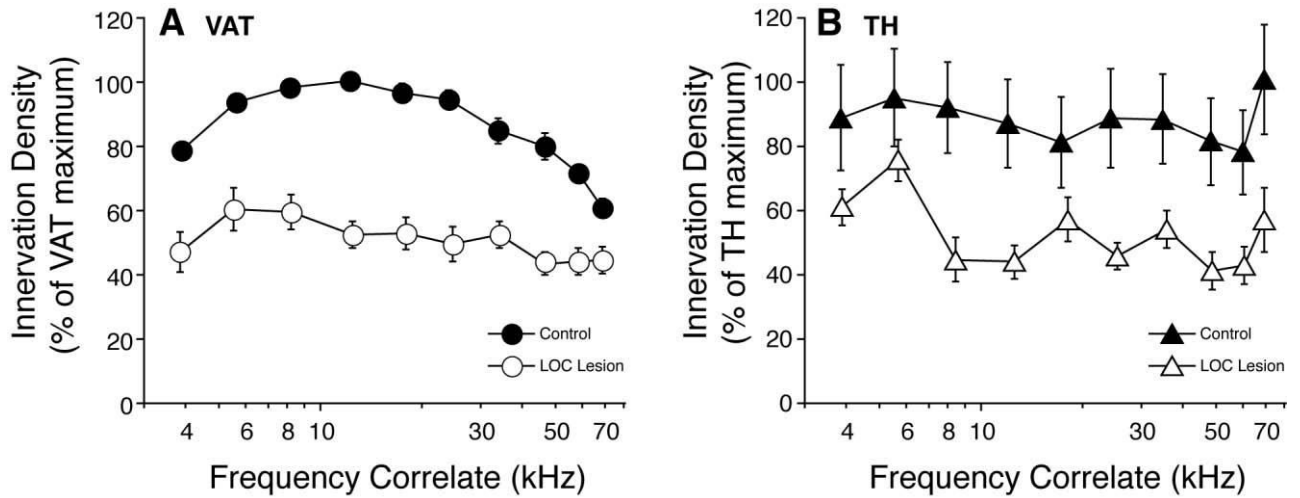


**Fig. 2.** Double immunostaining for TH (green) and VAT (red) in a confocal z-series shows lack of colocalization of these two transmitter markers. **A–C** show xy, xz, and yz projections, respectively. All projections suggest that there is minimal colocalization of TH and VAT in efferent terminals. None shows evidence for spatial segregation of TH- and VAT-positive terminals. **D–F** show isosurfaces viewed in the xy plane as generated by Amira 3-D visualization software: isosurfaces generated in 3-D enclose all voxels with signal intensity >90 in eight-bit images. Red surfaces were generated from the VAT signal, green from the TH signal. See text for further details. All images are from the same confocal z-stack (114 slices at 0.25  $\mu\text{m}$  per slice) from the lower second turn. Scale bar = 20  $\mu\text{m}$ .



**Fig. 3.** Comparison of xy projection (**A**) and a single slice (**B**) from a double-immunostained confocal z-series shows that apparent colocalization in the projection view (yellow arrows in A) often arises from superposition of signal from different focal levels and thus different terminals: the source of the green channel (TH) signal in A is shown by the arrows in B; at that focal level, there is no red (VAT signal). All images are from the same confocal z-stack (114 slices at 0.25  $\mu\text{m}$  per slice) from the middle of the second turn. Scale bar = 20  $\mu\text{m}$ .



**Fig. 4.**

Semiquantitative analysis of the density of VAT-positive (**A**) and TH-positive (**B**) terminals in the inner hair cell area shows that TH immunoreactivity in control ears is uniformly distributed along the cochlear spiral and that, after LOC lesion, both types of immunoreactivity decline to a similar degree. This analysis included 36 cochleas: the observer (blind to case history) separately rated the density of VAT-positive or TH-positive puncta on a four-point scale (see Materials and Methods) at 10 positions along the cochlear spiral in each case. These cochleas were from 17 animals with unilateral brainstem lesion; based on analysis of brainstem sections, the LOC cells were at least partially destroyed in 10 of 17 cases (“LOC lesion”). Control data are from the 17 opposite ears and two ears from animals without any brainstem surgery. Mean data ( $\pm$ SEM) are shown for each group, normalized for each immunostain by dividing by the maximal mean value for that stain.

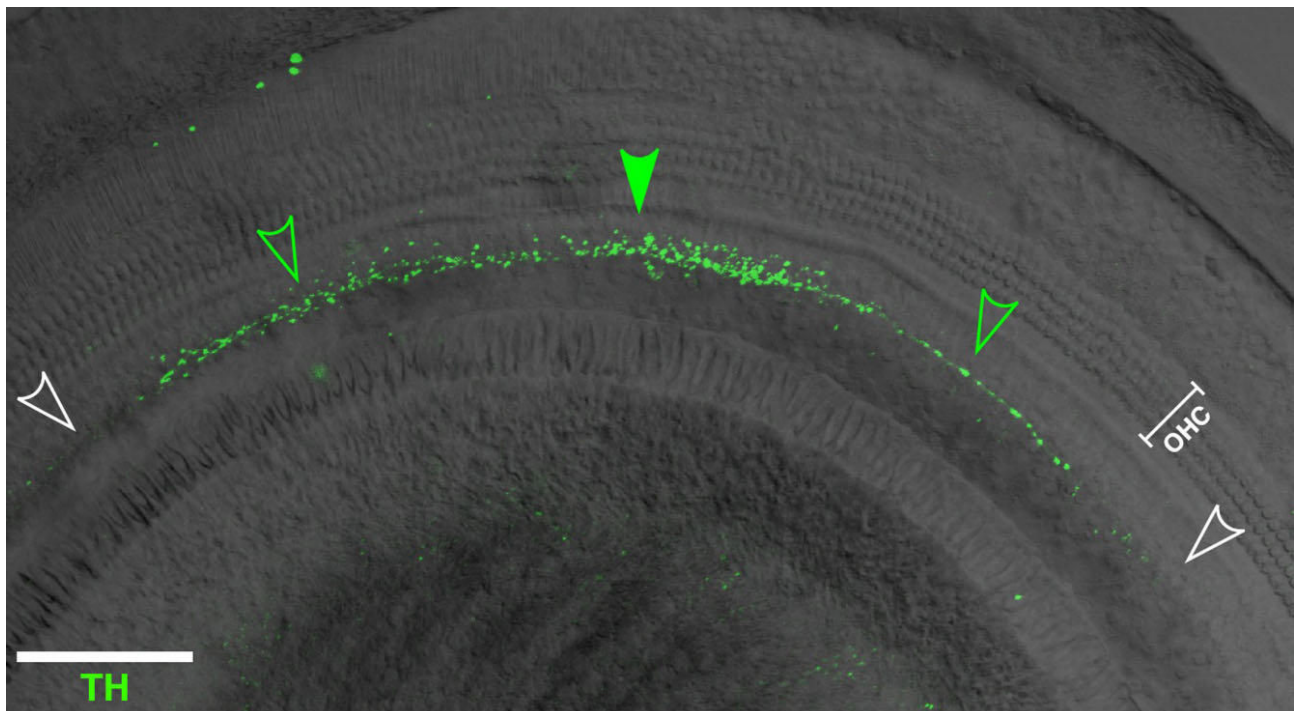


**Fig. 5.** Confocal image merging the TH signal (green) and the DIC image (gray scale) shows that TH immunoreactivity in the mouse cochlea is spotty: regions of the inner spiral bundle with high density of labeled terminals (solid green arrowhead) can be flanked by regions of low density (open green arrowheads) and, in turn, by regions with no immunostaining (white arrowheads). This image is the xy projection of a z-stack comprising 21 steps at 1.25- $\mu\text{m}$  steps from the upper basal turn. Scale bar = 100  $\mu\text{m}$ .

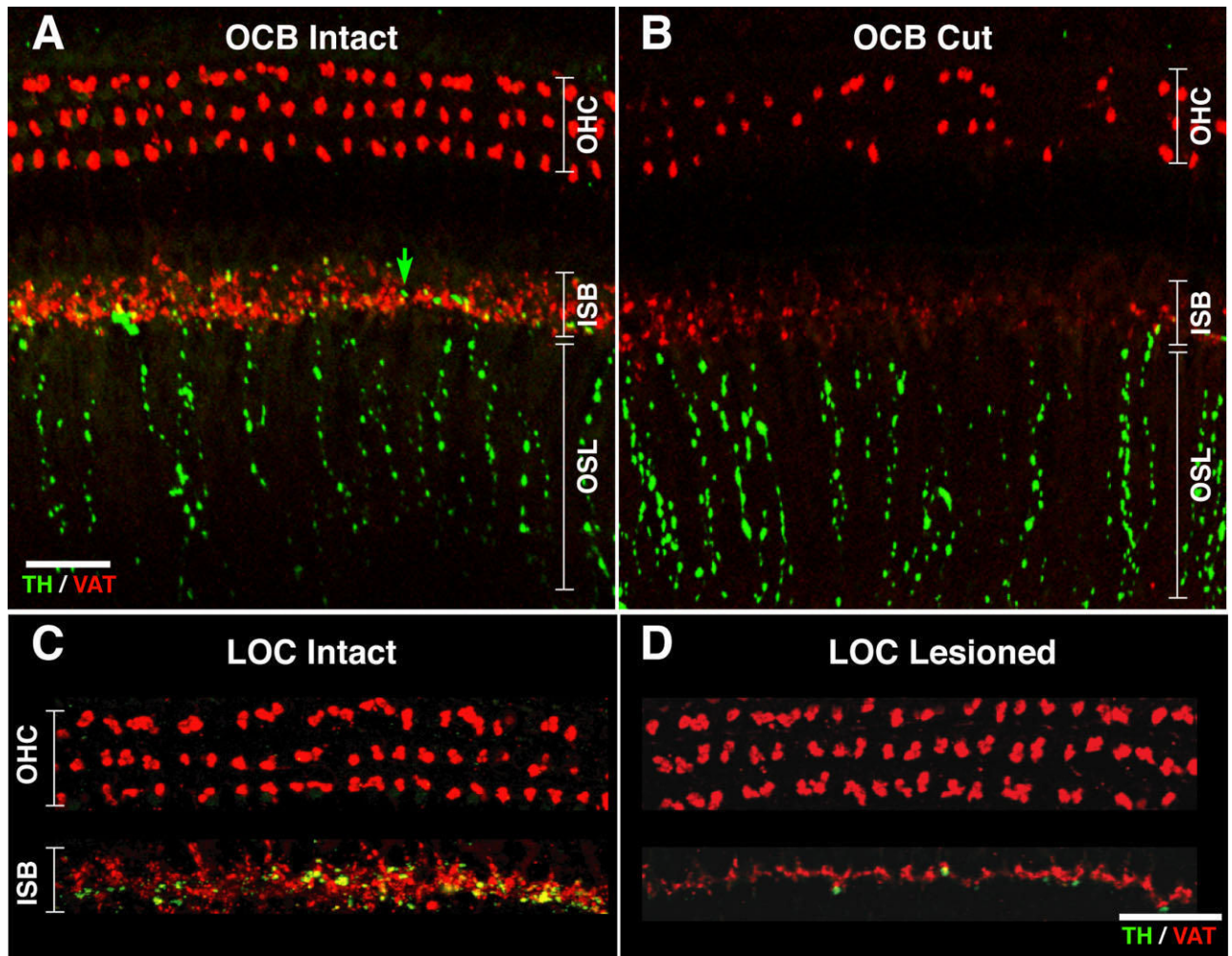


**Fig. 6.** Double immunostaining for TH (green) and VAT (red) in a control cochlea (**A,C**) and the opposite cochlea (**B,D**) after either section of the olivocochlear bundle (**B**) or injection of neurotoxin into the LSO (**D**). **A** is from a control cochlea showing a few TH-positive (green) swellings (e.g., arrow) among the VAT-positive (red) terminals in the inner spiral bundle (ISB). **B** is the place-matched cochlear region from the partially deafferented opposite ear, showing loss of VAT-positive terminals in ISB and outer hair cell (OHC) areas, loss of TH-positive terminals in the ISB area, and no obvious loss of TH-positive beaded fibers in the osseous spiral lamina (OSL). Both images are from the lower second turn and comprise xy projections of confocal z-series spanning 33–40  $\mu\text{m}$  of focal depth in 0.5- $\mu\text{m}$  steps. **C** shows TH and VAT immunostaining of the organ of Corti a control ear, whereas **D** shows the place-matched cochlear region from the opposite ear, which was ipsilateral to a neurotoxin injection that hit the LSO. Both images are from the upper basal turn and comprise xy projections of confocal z-series. Scale bars = 25  $\mu\text{m}$  in **A** (applies to **A,B**); 40  $\mu\text{m}$  in **D** (applies to **C,D**).

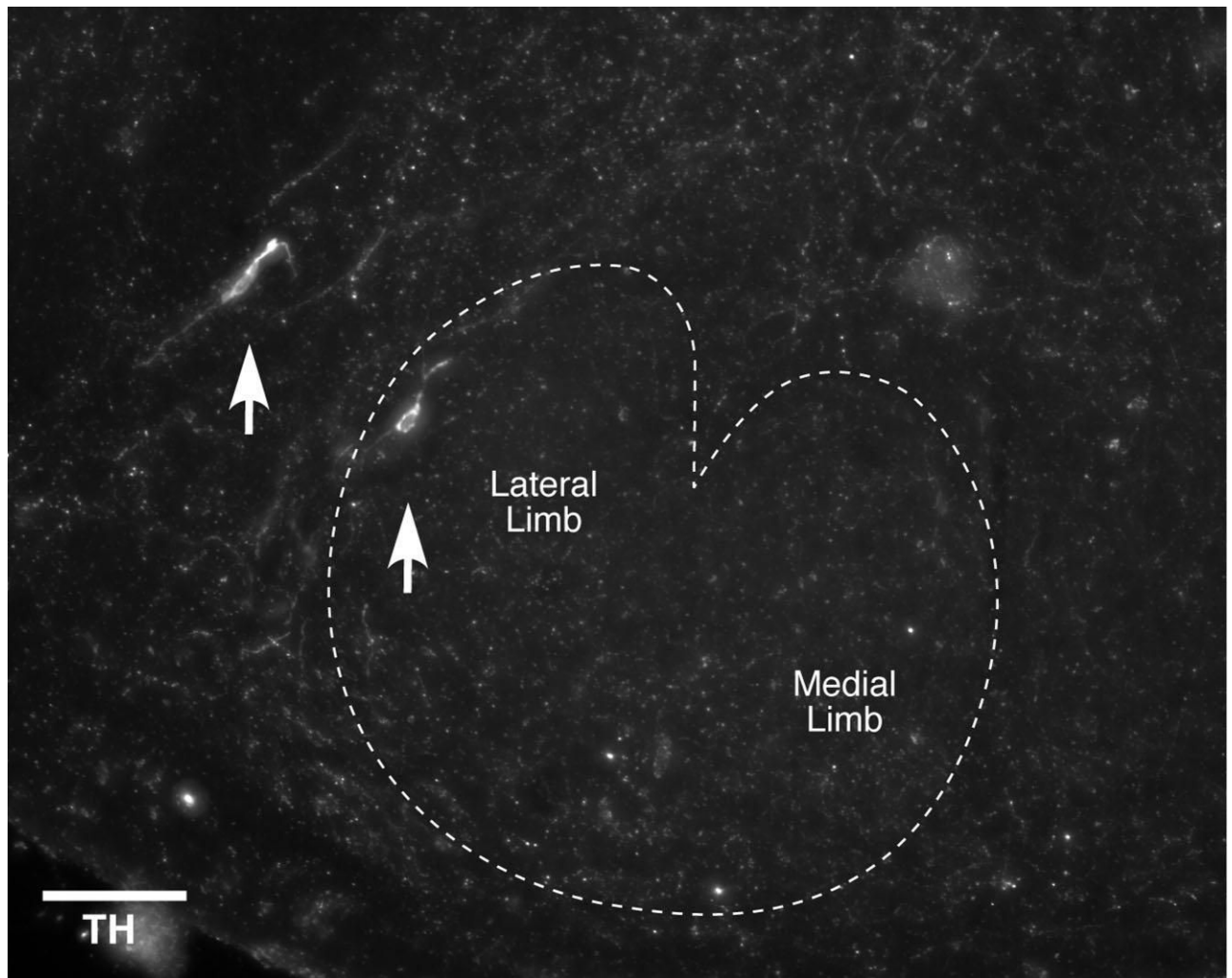


**Fig. 7.** TH-positive cell bodies (arrows) located within and around the LSO. An approximate outline of the LSO is indicated by the dashed line, and the locations of lateral and medial limbs are indicated. Image is an xy projection of a z-stack through one 15- $\mu$ m section acquired with a conventional light microscope (0.5  $\mu$ m/slice). Scale bar = 100  $\mu$ m.

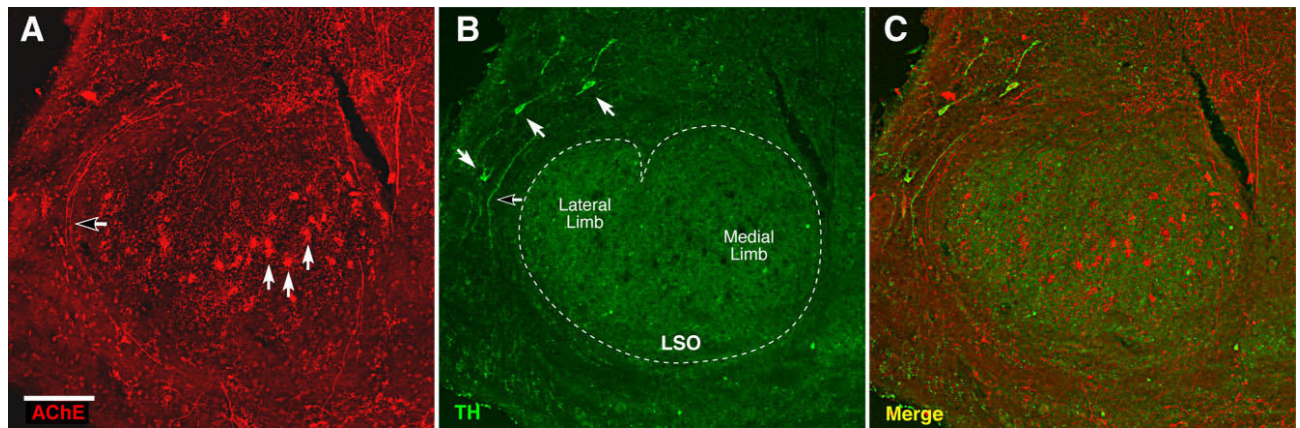


**Fig. 8.**

Double staining (AChE, red; TH, green) of brainstem sections through the superior olivary complex suggests that the TH-positive innervation of the cochlea arises from a separate population of noncholinergic neurons, in the “shell” around the LSO. **A** shows an AChE-stained section of mouse brain: solid arrows point to three of the many AChE-positive cholinergic neurons within the LSO. One of the many AChE-positive axons encircling the LSO is indicated by the open arrow. **B**: Three TH-positive cells (solid arrows) and one TH-positive axon (open arrow) are highlighted. **C**: Merge of images in A and B shows the complementary distribution of AChE and TH signal in both cell bodies and axons. The AChE was visualized with a histochemical stain producing a black reaction product; the TH was visualized with a fluorescent antibody. The AChE image is shown as red to simplify merging of the images. Scale bar = 100  $\mu\text{m}$ .